Siberian Branch of Russian Academy of Science
BUDKER INSTITUTE OF NUCLEAR PHYSICS

V.P. Bolotin, V.S. Cherkassky, I.K. Igumenov,
D.A. Kayran, B.A. Knyazev, E.I. Kolobanov,
V.V. Kotenkov, V.V. Kubarev, G.N. Kulipanov,
G.L. Kuryshev, A.N. Matveenko, L.E. Medvedev,
S.V. Miginsky, L.A. Mironenko, A.D. Oreshkov,
V.K. Ovchar, A.K. Petrov, V.M. Popik,
T.V. Salikova, S.S. Serednyakov, A.N. Skrinsky,
O.A. Shevchenko, M.A. Scheglov, N.A. Vinokurov,
N.S. Zaigraeva

STATUS OF THE NOVOSIBIRSK FREE ELECTRON LASER AND FIRST EXPERIMENTS WITH HIGH POWER TERAHERTZ RADIATION

Budker INP 2004-57

Novosibirsk
2004

V.P. Bolotin[1], V.S. Cherkassky[2], I.K. Igumenov[3], D.A. Kayran[1],

B.A. Knyazev[1], E.I. Kolobanov[1], V.V. Kotenkov[1], V.V. Kubarev[1], G.N. Kulipanov[1], G.L. Kuryshev[4], A.N. Matveenko[1], L.E. Medvedev[1], S.V. Miginsky[1], L.A. Mironenko[1], A.D. Oreshkov[1], V.K. Ovchar[1], A.K. Petrov[5], V.M. Popik[1], T.V. Salikova[1], S.S. Serednyakov[1], A.N. Skrinsky[1], O.A. Shevchenko[1], M.A. Scheglov[1], N.A. Vinokurov[1], N.S. Zaigraeva[1]

Status of the Novosibirsk free electron laser and first experiments with high power terahertz radiation

[1] Budker Institute of Nuclear Physics 6300906, Novosibirsk, Russia

[2] Novosibirsk State University (NSU), 630090 Novosibirsk, Russia.

[3] Institute of Non-organic Chemistry SB RAS, 630090 Novosibirsk, Russia.

[4] Institute of Semiconductor Physics SB RAS, 630090 Novosibirsk, Russia.

[5] Institute of Chemical Kinetics and Combustion SB RAS, 630090 Novosibirsk, Russia.

Abstract

The first stage of Novosibirsk high power free electron laser (FEL) was commissioned in 2003. Now the FEL generates electromagnetic radiation in the wavelength range 120 – 180 micrometers as a continuous sequence of 50-ps pulses following with the repetition rate of 5.6 MHz at the average power up to 200 W (the peak power – 0.6 MW). The measured relative linewidth is 0.3%, which is close to the Fourier-transform limit. Recently constructed 13-m transmission line transports laser radiation out of the radiation-dangerous zone to the user-station hall. A number of experiments have been carried out on the first user station. We obtained first continuous optical discharge sustained by THz radiation in argon and air of atmospheric pressure, as well as ablation of PMMA in the argon buffer gas. We have developed several techniques for the visualization of high-power submillimeter radiation and performed, using these techniques, classic optical experiments, including lensless Fourier holography. Wide variety of experiments with application of THz radiation to physics, chemistry, biology and technology are under consideration. The prospects for the Novosibirsk FEL as a user facility are discussed.

Index Terms—Free electron laser, accelerator-recuperator, terahertz radiation, submillimeter radiation, continuous optical discharge, laser ablation, terahertz imaging, holography

Corresponding author e-mail: knyazev@inp.nsk.su).

и первые эксперименты с мощным терагерцовым излучением

В. Р. Болотин[1], В. С. Черкасский[2], И К. Игуменов[3], Д А. Кайран[1], Б А Князев[1], Е И. Колобанов[1], В. В Котенков[1], В В Кубарев[1], Г. Н. Кулипанов[1], Г. Л. Курышев[4], А. Н. Матвеенко[1], Л. Е. Медведев[1], С. В. Мигинский[1], Л. А. Мироненко[1], А. Д. Орешков[1], В. К. Овчар[1], А. К. Петров[5], В. М. Попик[1], Т. В. Саликова[1], С. С. Середняков[1], А. Н. Скринский[1], О. А. Шевченко[1], М. А. Щеглов[1], Н. А. Винокуров[1], Н. С. Заиграева[1]

[1] Институт ядерной физики им. Г.И. Будкера СО РАН, 630090 Новосибирск
[2] Новосибирский государственный университет, 630090 Новосибирск
[3] Институт неорганической химии СО РАН, Новосибирск
[4] Институт физики полупроводников СО РАН, Новосибирск
[5] Институт химической кинетики и горения СО РАН, Новосибирск

Аннотация

Первая очередь Новосибирского лазера на свободных электронах (ЛСЭ) была запущена в 2003 году. В настоящее время ЛСЭ генерирует электромагнитное излучение в диапазоне длин волн 120 – 180 мкм в виде непрерывной последовательности 50-пикосекундных импульсов, следующих с частотой повторения 5.6 МГц, при средней мощности 200 Вт (пиковая мощность – 0.6 МВт). Измеренная относительная ширина линии равна 0.3%, что близко к пределу, определяемому преобразованием Фурье. Недавно смонтированный 13-метровый транспортный канал передает излучение лазера из радиационно-опасной зоны в помещение, предназначенное для рабочих станций пользователей. На первой временной рабочей станции выполнен ряд экспериментов. Впервые получен непрерывный оптический разряд в аргоне и воздухе атмосферного давления, поддерживаемый терагерцовым излучением. Наблюдалась также интенсивная абляция оргстекла в буферном газе (аргон). Разработано несколько методов визуализации мощного субмиллиметрового (терагерцового) излучения. Используя эти методы, выполнены эксперименты по классической оптике, включая безлинзовую фурье-голографию. Рассматриваются возможные эксперименты с использованием мощного терагерцового излучения в исследованиях по физике, химии, биологии, технологии и др. Обсуждаются планы создания рабочих станций пользователей.

I. Introduction

Exponentially growing number of publications devoted to development of THz sources and applications of THz radiation reflects the expectation of a breakthrough to new technologies based on the radiation in this spectral range [1].

Appearance of new THz sources, which enable the resonance excitation of complex chemical and biological molecules, generated special interest to this spectral region. Most of the THZ sources generate broadband radiation with very low power. Conventional narrowband sources also have rather low power. Very intense terahertz radiation can be obtained with free electron lasers (FEL). There already exist several FELs generating radiation in this spectral range. Most of them have high peak power but the average power is less, some time substantially, than one Watt. Recently commissioned in Jefferson Lab sub-picosecond terahertz source [2] generates broadband radiation with the flux of 10 W/cm^{-1} in the spectral range 1 – 20 cm^{-1}.

A new narrowband Novosibirsk THz free electron laser was commissioned in 2003 [3]. It is CW FEL based on an accelerator–recuperator, or an energy recovery linac (ERL). It differs from the earlier ERL-based FELs [4, 5] in the low frequency non-superconducting RF cavities and longer wavelength operation range. The terahertz FEL is the first stage of a bigger installation, which are to be built in the following years and will provide shorter wavelengths and higher power.

Now the Novosibirsk terahertz FEL generates coherent radiation in the spectral range from 120 to 180 μm. The output radiation with the average power of about 200 W is now available for users at the first workstation. The radiation follows as a continuous sequence of 50-ps pulses with the pulse repetition rate of 5.6 MHz (it will be increased soon to 22.5 MHz). Maximum peak power is now 0.6 MW. The average spectral power density is about 600 W/cm^{-1}. In this paper, we briefly describe free electron laser characteristics, first experiments with THz radiations, and discuss plans for future user station development.

II. Novosibirsk free electron laser

A. Accelerator-recuperator

Full-scale Novosibirsk free electron laser is to be based on a four-orbit 50 MeV electron accelerator-recuperator (see Fig. 1). It is to generate radiation in the range from 3 micrometer to 0.2 mm [6, 7]. The first stage of the machine contains a full-scale RF system, but has only one orbit. Layout of the accelerator–recuperator

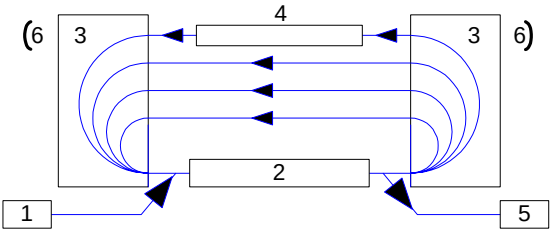

Fig. 1. Scheme of the accelerator-recuperator based FEL: 1 – injector, 2 – accelerating RF structure, 3 – 180-degree bends, 4 – undulator, 5 – beam dump, 6 – mirrors of optical resonator.

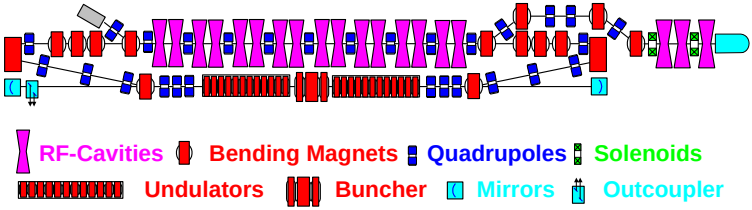

Fig. 2. Scheme of the existing accelerator-recuperator based terahertz FEL.

is shown in Fig. 2 and its general view in Fig. 3. The 2 MeV electron beam from an injector passes through the accelerating structure, acquiring 12 MeV energy, and comes to the FEL, installed in the straight section. After interaction with radiation in the FEL the beam passes once more through the accelerating structure, returning

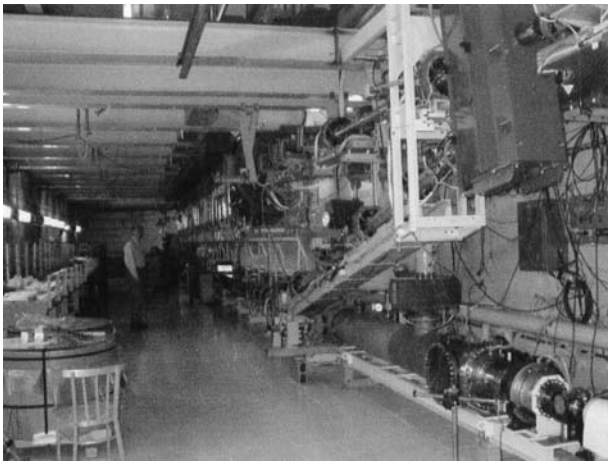

Fig. 3. General view of the accelerator-recuperator with undulator and one of the mirror assemblies.

the power, and comes to the beam dump at the injection energy. Main parameters of the accelerator are listed in Table 1.

Table 1. Accelerator parameters (first stage)

Quantity	Magnitude
RF frequency	180 MHz
number of RF cavities	16
amplitude of accelerating voltage at one cavity	0.7 MV
injection energy	2 MV
final electron energy	12 MeV
maximum bunch repetition rate	22.5 MHz
maximum average current	20 mA
normalized beam emittance	20 mm·mrad
final electron energy spread	0.2%
final electron bunch length	0.1 ns
final peak electron current	10 A

The FEL is installed in a long straight section of a single-orbit accelerator-recuperator. It consists of two undulators, a magnetic buncher, two mirrors of the optical resonator, and an outcoupling system. Both electromagnetic planar undulators are identical. The length of each undulator is 4 m, period is 120 mm, the gap is 80 mm, and deflection parameter K is up to 1.2. One can use one or both undulators with or without the magnetic buncher. The buncher is simply a three-pole electromagnetic wiggler. It is necessary to match the electron phases in undulators and is used now at low longitudinal dispersion $Nd < 1$.

Both laser resonator mirrors are identical, spherical, 15 m curvature radius, made of gold plated copper and water-cooled. In the center of each mirror there is an opening. It serves for mirror alignment (using He-Ne laser beam) and output of small amount of radiation. Both the mirrors have circular openings: 8 mm in diameter in the front (left) mirror, and 3.5 mm in diameter in the rear one.

B. Radiation study

For FEL operation we employed both undulators. Beam average current was typically 8 mA at repetition rate 5.6 MHz, which is the round-trip frequency of the optical resonator and 32-th subharmonics of the RF frequency $f \approx 180$ MHz. Instead of fine tuning of the optical resonator length we tuned the RF frequency. The tuning curve is shown in Fig. 4. The radiation wavelength was tuned in the range 120 – 180 micrometers depending on the undulator field amplitude. The shortest wavelength is limited by the gain decrease at a low undulator field, and the longest one – by the optical resonator diffraction loss increase. The minimum relative linewidth (FWHM), measured with Fabri-Perot etalon, was near $3 \cdot 10^{-3}$.

The corresponding coherence length $\lambda^2/(2\Delta\lambda) = 2$ cm is close to the electron bunch length, therefore we, obviously, close to the Fourier-transform limit.

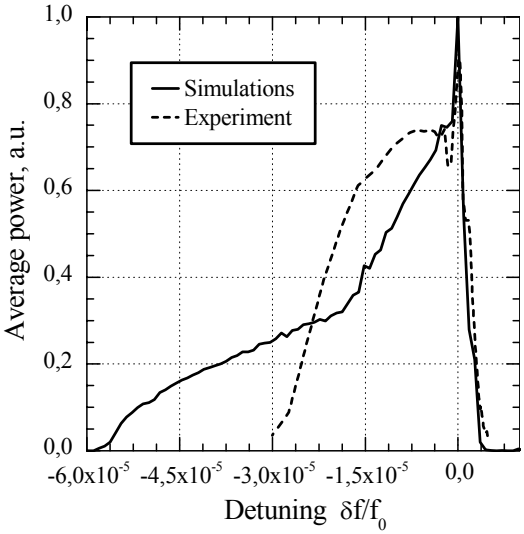

Fig. 4: Dependence of the average power on the RF frequency detuning.

Table 2. Radiation parameters

Quantity	Magnitude
wavelength	0.12...0.18 mm
minimum relative linewidth, FWHM	0.003
pulse length, FWHM	50 ps
peak power	0.4 MW
repetition rate	5.6 MHz
average power	0.2 kW

The loss of the optical resonator was measured with a fast Schottky diode detector [8]. Switching off the electron beam, we measured the power decay time. The average radiation power, emerging through the opening in the front mirror, is close to 200 W. The typical round-trip loss value is about 7%. Consequently, approximately 1 kW of electron beam power is converted to the coherent radiation. Since the electron beam power is 100 kW, the system efficiency is about 1%. The typical radiation parameters are listed in Table 2. The average spectral power density is about 600 W/cm^{-1}. Both the average power and the average spectral power density of the laser are the highest ever obtained in the submillimeter spectral range.

III. High power density experiments

A. Continuous optical discharge in submillimeter range

For the demonstration of capabilities of the laser as a high-power THz source the laser beam was focused with an on-axis parabolic mirror ($f = 10$ mm) in the atmospheric pressure argon or air directly at the output of the laser. Preliminary estimation of the optical breakdown threshold, made in accordance with [9], showed that even for maximum possible power density $F_{peak} \approx E_{pulse} / \lambda^2 \tau$, where τ is a pulse length, we cannot reach the threshold. Nevertheless, we have obtained the continuous optical discharge for both gases. Fig. 5 demonstrates the photography of the parabolic mirror with the discharge at the focal point. The glares on the mirror surface are merely the reflection of the plasma luminosity off the mirror.

Fig. 5. The continuous discharge in the focus of the parabolic mirror.

There may be a number of reasons, why the breakdown occurs at a lower power density than the theory predicts. First of all the theory is developed for the sparks produced by a single laser shot. High repetition rate of continuously following pulses makes, probably, possible initiation of the breakdown due to statistical reasons (occasional appearance in the focus of a number of initial electrons sufficient for spark initiation). Being once produced, the plasma ball has no time to recombine or expand between the laser pulses and this provides farther discharge sustaining. The other reasons may be inapplicability of the theory for the picosecond pulses or the effect of background X-rays, because this experiment had been carried out inside the accelerator hall. Further study of the continuous optical discharge in the THz spectral range can bring an advance in our understanding of this phenomenon.

B. Laser ablation

Other demonstration of high intensity of the THz laser radiation is ablation of PMMA. A PMMA parallelepiped was placed at a distance of 30 cm in front of the laser output mirror. An argon flow removed the air from the crater and prevented PMMA burning. The video film demonstrates fast ablation of the PMMA block without combustion. Resulting conical opening is shown in Fig. 6, where the space between the graduation marks is equal to 5 mm. Since the combination of radiation intensity and the pulse length critically affect on the ablation process (see, e. g., [10]), the study of the ablation products will be one of the first experiments on the facility.

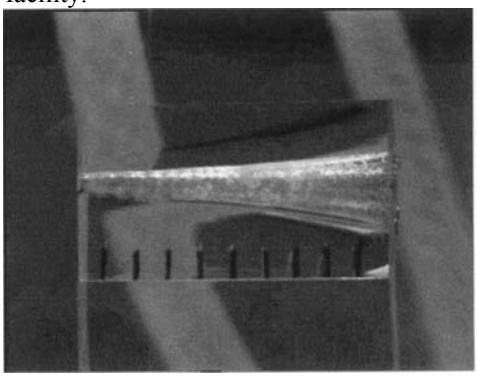

Fig. 6. The conic hole drilled in the PMMA parallelepiped via ablation by terahertz radiation. One division is 5 mm.

IV. Optical beamline and first user station

To transmit the radiation from the front mirror to user stations, a 13-m beamline guiding THz radiation from the accelerator hall to the user rooms had been constructed. Since the water vapor has a great number of absorption lines in the submillimeter spectral range, the beamline is isolated from the atmosphere and filled out with dry nitrogen. The nitrogen pressure is sustained to be equal to the atmospheric pressure. The beamline is separated from the accelerator vacuum by a 0.6-mm diamond window.

In the close future the beamline will be continued to several stationary user stations. Temporary, the beamline output is separates from the atmosphere with a polyethylene film and directed with a plane mirror to the first user station. In future this station will be employed for monitoring laser beam characteristics and for spectroscopy (see sect. VII) and will be further referred as the “metrology station”. The station is supplied with an optical bench, pyroelectric detectors and other equipment. It is to be also isolated from the atmosphere, but all the experiments described below were performed without isolation. In these

experiments the wavelength was not monitoring (generation wavelength, linewidth and tuning range were studied in special experiments previously [3] – see Table 2). To escape strong radiation absorption, we tuned in each experiment the laser wavelength to a wavelength, where the absorption at the distance up to two meters was negligible. With the accuracy sufficient for simple estimations one can assume the wavelength to be equal to 0.15 mm.

V. Imaging techniques for high power THz radiation

Imaging in the terahertz spectral range is a subject of special interest for many applications such as medicine, biology, industry, security and so on. Recently developed methods for terahertz imaging (see, *e.g.*, [11]) are based on the employment of the wideband or narrowband low-power THz sources. Due to low power of these sources the visualization of images requires the employment of rather sophisticated detectors, and, in most cases, recording an image takes quite a while.

High power of our laser enables application for the visualization of laser radiation the methods, which, probably, sometime were used for intense visible and NIR radiation, but were never previously employed in the terahertz range. We employed for the visualization two methods based on thermal effect of intense terahertz radiation.

A. Visualization with a FIR-NIR converter

This technique, further referred as FNC, employs temperature growing of a thin-film screen exposed to terahertz radiation (Fig. 7). Two-dimensional field of temperature at the screen surface is recorded with a thermograph SVIT, which have a 128×128 InAs focal plain array (FPA) sensitive to the radiation within the spectral range of 2.6 – 3.1 μm. Thermograph sensitivity at the room temperature is 0.03 ºC at the frame frequency up to 40 Hz. In our case time resolution was restricted by thermal relaxation of the thermoconverter and the frame frequency in the experiments was 10 Hz.

In the first experiments the carbon paper was used as a thermoconverter. Fig. 7 demonstrates the image of keys put into a dense paper envelope, which is transparent for THz radiation. The other picture is a frame of the video film recorded with the thermograph when the aluminum mask with a set of openings forming the letters “FEL BINP” placed in front of the screen. Moving the mask we observed that characteristic thermal relaxation time for the carbon paper was 1 – 2 seconds.

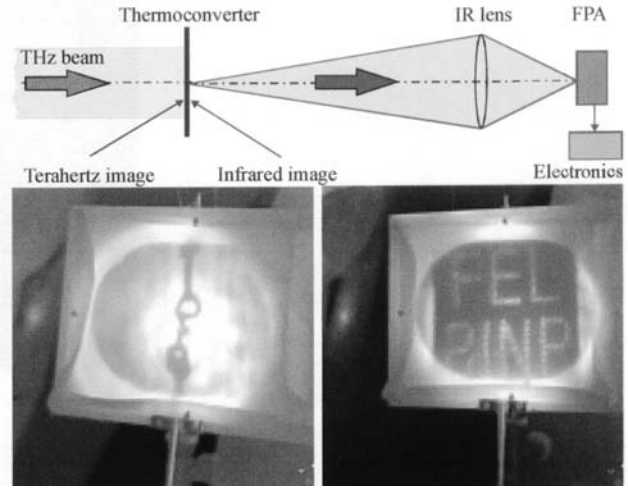

Fig. 7. Schematic layout of the FIR-NIR converter and the snapshots of THz images: keys in the paper envelope and the image recorded when a metal mask with 3-mm holes drilled with a step of 6 mm was placed in front of the thermoconverter.

B. Visualization with the thermo-optical detector

The other technique used for the visualization of terahertz images was the Thermo-Optical Detector (TOD). The technique employs the change of the optical length of a medium, which is transparent for probe visible light but is opaque for the terahertz radiation, when the medium is exposed to terahertz radiation. The change of the optical length within the expose time τ is

$$\Delta S \equiv \frac{\partial S}{\partial t}\tau = \Delta\left(\int_L n(z,T(t))\,dz\right), \qquad (1)$$

where z is the coordinate across the medium slab and T is a local temperature. The difference occurs because of both the thermal expansion and the change of the refraction index for the heated portion of the medium. Corresponding phase shift for a single pass with the accuracy to the members of second order infinitesimal can be written [12] as

$$\Delta\varphi\left(x,y\right) = \frac{\psi}{\lambda}\cdot Q(x,y)\,, \qquad (2)$$

where $Q(x,y)$ is an areal distribution of the specific energy density absorbed in the medium and λ is a wavelength of the probe (visible) radiation. The value

$$\psi[\mathrm{cm}^3/\mathrm{J}] = 2\pi(\beta+\alpha n)/\rho c_p \qquad (3)$$

(here $\beta = dn/dT$, α, ρ and c_P are a coefficient of thermal expansion, a specific

density and a specific heat at constant pressure) is a constant for each optical material. Recording the phase shift, one easy finds the energy density distribution.

We have considered several variants of this technique [13]. The variant that was verified experimentally (Fig. 7) employs the interference of two wavefronts of visible coherent light reflected from two surfaces of a parallel-sided (or wedged) glass plate. We used a 20-mW semiconductor laser ($\lambda = 650$ nm) with a lens system as a source of the plane wave. The interference pattern recorded before the expose of the plate to THz radiation was used as a reference one. After that the plate was exposed to the radiation that is absorbed in the plate (we used both KrF-laser ultraviolet radiation and free electron laser THz radiation) and the diffraction pattern gradually changed because of the thermo-optical effect.

The phase shift of the wave reflected from the rear (exposed to the radiation under study) glass surface obeys the equation (2). Phase shift at each point $2\Delta\varphi\left(x, y\right) = 2[\varphi(\tau) - \varphi(0)]$ is proportional directly to the energy density, deposited into the plate, which can be written as

$$E(x, y; t) = \Delta N(x, y; t) \cdot K \,. \tag{4}$$

Here ΔN is the fringe shift (generally speaking it is a real but not an integer value) and K is a proportionality factor

$$K = \lambda \rho c_p / 2(\beta + \alpha n) \,, \tag{5}$$

where λ is a probe light wavelength and factor 2 appears because the probe wave passes the plate twice. For the inclined reference beam one needs in addition to take into account the dip angle.

Factor $K \approx 4.0$ J/fringe·cm^2 for a light glass. Sensitivity of the technique can be increased if one uses a material with higher thermo-optical constant ψ (see Eq. (3)). For example, for PMMA factor $K \approx 0.44$ J/fringe·cm^2 [12]. Thus, the described technique enables direct measurement of the energy density distribution. Time resolution of the technique depends on the expose time and method of the heat sink. Without special cooling and for shot radiation pulses (40-ns pulse of KrF laser) initial interference pattern resumes its original shape in about one second after the pulse. For long expose time, when the heat penetrates deep into the plate, the relaxation time noticeably grows. For the materials with high thermo-optical coefficient and with adequate cooling one can expect to obtain, for a detector system with a shutter, recording with the frequency of about 10 frames per second. We consider also the possibility to use liquid targets.

The interferograms in Fig. 8 demonstrate application of the TOD to recording THz-laser beam cross-section at the output of the beamline (13 meters from the laser output mirror). These interferograms can be interpreted as two frames at the holographic interferometry. Numerical reconstruction of digitally recorded holograms enables to escape the stage of real superimposition of the interferograms and to retrieve the phase difference distribution with a simple

digital procedure [14]. It becomes to be possible because the digital reconstruction of hologram, in contrast to the optical reconstruction, enables to obtain both amplitude and phase of the retrieved wavefront. Methods for interferogram processing are well-known and the TOD imaging system working in real time with a high repetition rate does not seem to be impossible.

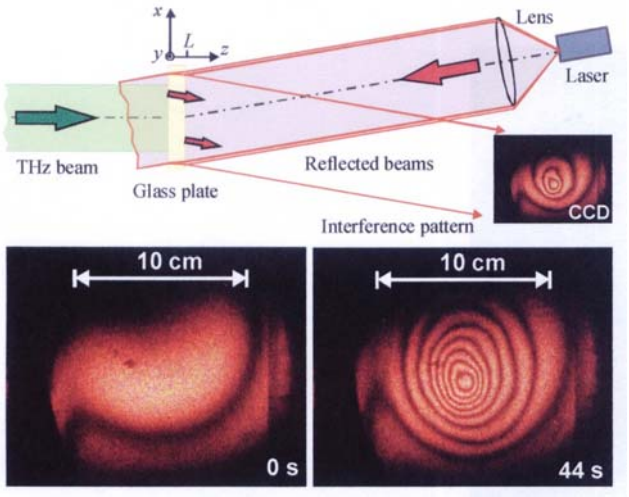

Fig. 8. Schematic layout of the thermo-optical detector (TOD) and the snapshots taken with a digital video camera: the reference interference pattern (on the left) and the image recorded after exposition of the parallel-sided glass plate with THz laser beam during 44 seconds.

Fig. 9 demonstrates the THz beam cross-section taken with FNC (on the left) and TOD (on the right) techniques. The results reveal reasonable agreement between the cross-sections, and their profiles are close to the profile recorded with a pyroelectric transducer.

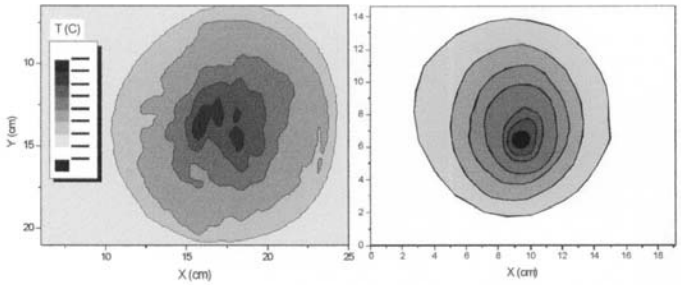

Fig. 9. THz beam cross-sections recorded with FNC (on the left) and TOD. The last image is retrieved from "mirror-reflected" interferogram of Fig. 7, in this case both figures shows the beam cross-section as it is seen at the beamline output.

The TOD technique was also used for visualization of a fine detailed THz image (Fig. 10). To form this image THz radiation came through the mask in the aluminum plate, shown in Fig 11, which had shape of the letter "K" surrounded with an annular aperture. The width of all the apertures was about 3 mm. The mask was places directly in front of the glass plate and the diffraction effect was negligible.

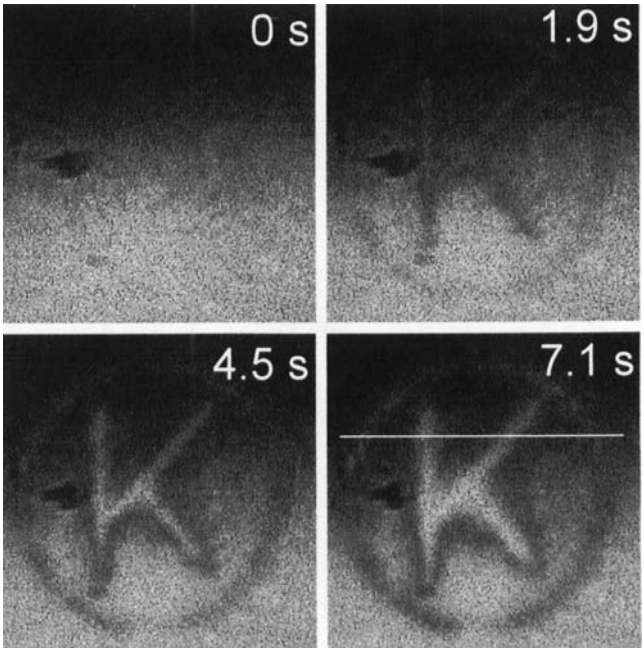

Fig. 10. Sequence of images recorded with the TOD technique (see Fig. 8). THz laser radiation passed through the aperture (see photography in Fig. 11) and was absorbed in the glass plate.

One can see from Fig. 10 that the interference method enables to obtain undistorted terahertz images when the phase shift is less than 2π. In opposite case, the interference pattern appears in the image, but shape of the image is still visible clearly. The image blurs with time due to the thermal relaxation. Since the energy distribution of the terahertz beam is close to the Gaussian one, energy deposition in the ring is less than in the center of the image, and, respectively, spreading of the ring occurs slower than spreading in the center of the image. Fig. 12 illustrates this fact. It is evident, and special experiments with 20-ns KrF laser corroborated it, that for shot pulses one can obtain undistorted images using a thermal screen with an adequate cooling system.

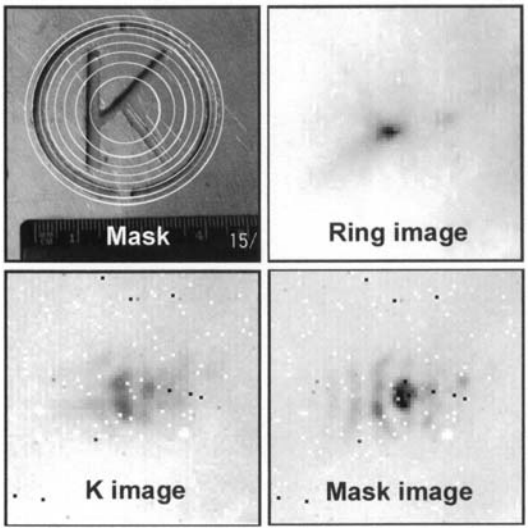

Fig. 11. Photography of the mask with “K and ring” aperture and the diffraction patterns recorded with the thermograph at a distance of 180 cm for partially shaded and completely open aperture. White rings drawn on the mask show the Fresnel zones observing from this distance.

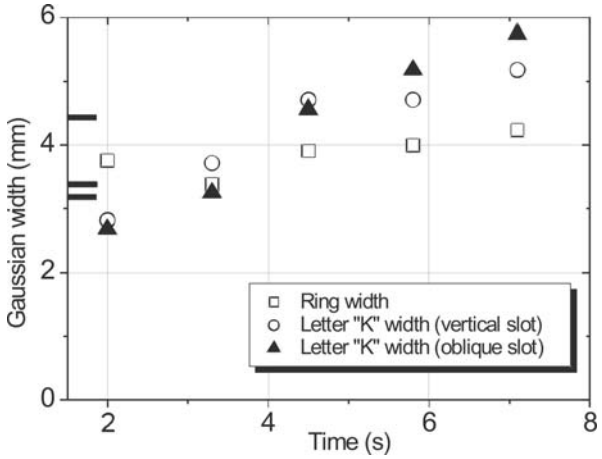

Fig. 12. Gaussian width vs. time for the stripes in the THz image formed with “K and ring” aperture (see Fig. 11) and recorded with the TOD technique. Width profiles were plotted for the trace marked with white line in Fig. 9. The geometrical widths of the slots are shown at the abscissa axis. Some points at the beginning of the curves have very high dispersion due to small noise/signal ratio originated from the speckle effect.

Since measurement of power density, as well as visualization of terahertz radiation, are a subject of high importance for most of future experiments, we will continue the development of these two techniques and consider the other possible methods like the fluorescence board, pyroelectric and Goley-cell matrices and so forth.

VI. Classical optic experiments

Photon energy of the submillimeter radiation is about 10 meV. Most of phenomena in this spectral range can be described with excellent precision by the classical optics theory. To demonstrate high transverse and longitudinal coherence of the FEL radiation, we carried out a number of experiments on classical optics.

A. Interference and diffraction

The transverse coherence of the free electron laser radiation was clearly demonstrated by classical interference pattern recorded with the thermograph when two large aluminum mirrors, positioned at a small angle, reflected the laser beam on the carbon-paper screen placed at the distance of 180 cm. In the next experiment we recorded Fresnel diffraction on the mask shown in Fig. 11. In contrast to diffraction experiments in the visible spectral range, for the submillimeter range characteristic dimension of apertures are to be of millimeter or centimeter order of value. Outer diameter of the ring-shape opening in the aperture shown in Fig. 11 is 42 mm. The mask contains seven Fresnel zones for the distance of 180 cm. Since the ring itself contains only one Fresnel zone, its diffraction pattern is a Poisson's spot (right upper picture in Fig. 11). The diffraction pattern of the K-aperture is, as one can expect, contains three main spots corresponding to three slots. Whole aperture produces more complex diffraction pattern shown in the right lower frame.

Next diffraction experiment with two circular apertures enables compare calculated diffraction pattern with the pattern recorded with the thermograph. Two openings were 6 mm in diameter and spaced in horizontal direction at a distance of 14 mm. The screen was placed at the same distance as in the previous experiment. The diffraction pattern at the distance of 108 cm is shown in Fig. 13, *a*. The ratio of initial intensity of THz radiation at the openings was 9:20 (see Fig. 13, *b*).

Experimentally recorded and calculated intensity profiles of the pattern are plotted in Fig. 13, *c*. In the calculation we took in account the difference in intensities. In the scope of this experiment the radiation may be considered as completely monochromatic. One can see that the positions and relative intensities perfectly correlate for calculated and recorded peak profiles. We concluded from the numerical simulation that the wavelength of laser radiation in this experiment was 160 μm. This method for the determination of radiation wavelength in the THz spectral range seems to be very simple and reliable, and, obviously, can be

used for regular monitoring of THz-laser wavelength.

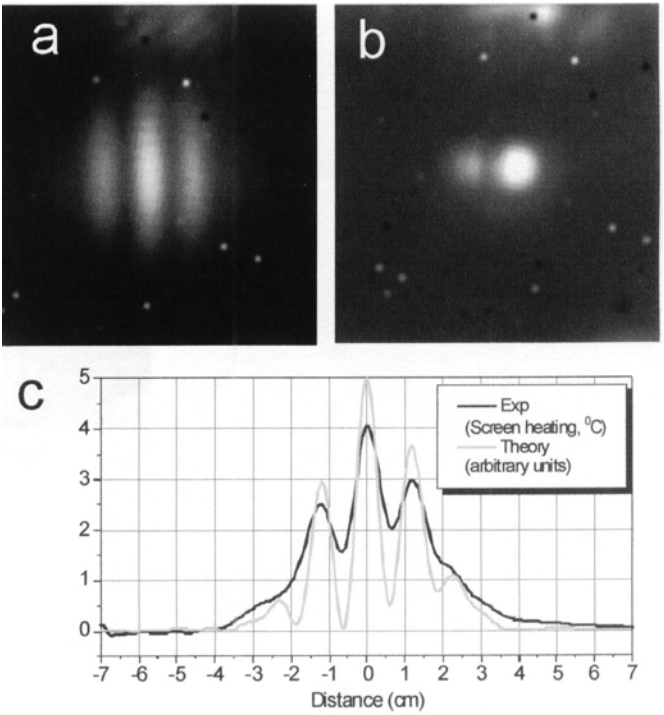

Fig. 13. The diffraction pattern (*a*) produced by two circular apertures (*b*), $\varnothing = 6$ mm, Δ = 14 mm, is recorded by the thermograph. The carbon paper screen was placed at a distance of 108 cm. The plot (*c*) shows experimentally observed and theoretically calculated intensity profiles. The theoretical curve was calculated for $\lambda = 160$ μm.

The peak widths in the experimental profile are wider (and, as a consequence, the fringe visibility is less) than in the calculated one. Apparently, it is a consequence of thermal relaxation over the screen surface. The peak broadening enables to estimate the spatial resolution as 2 – 3 mm for quasi-CW irradiation. Obviously, using a shutter in the combination with screen cooling allows increasing spatial resolution.

B. Terahertz holography

High radiation intensity of the Novosibirsk free electron laser opens the real opportunity for holography in the terahertz spectral range. It seems to be not possible with the conventional THz sources for at least three reasons. First, most of the sources are not monochromatic. Second, the monochromatic sources have

very low intensity, and there are no materials for recording of such radiation. Third, for obtaining acceptable resolution a hologram has to have sufficient number of resolving elements [15]. Because of large wavelength of the THz radiation in can be done only if the area, where the hologram is recorded, is sufficiently large.

Evidently, our free electron laser has the capability for development of holography techniques and it will be one of the directions for future experiments. The diffraction patterns presented in Figs. 12 and 13 are already, in fact, the simplest holograms. For example, the letter "K" in the mask Fig. 11 may be interpreted as an object and the annular aperture plays a role of the reference source. Whole diffraction pattern in this case is a hologram. It is clear that such "lensless Fourier hologram" [15] in Fig. 11 is a very primitive one and has limited number of "interference fringes".

We applied the method of numerical reconstruction of digitally recorded holograms [14] to this hologram and to the "hologram" shown in Fig. 13, *a*. As we expected, quality of the reconstructed images was very poor, but the reconstruction have demonstrated the main features of such kind of hologram and the feasibility of holography in the terahertz spectral range. The next goal for our experiments will be recording holograms in the geometry which enables reconstructing THz images with high resolution. Development of terahertz holography may sufficiently enlarge capability of the terahertz imaging.

VII. User workstations on the THz FEL

At present time, the main efforts are directed to design and construction of user stations. Following stations are to be created in the collaboration with research institutes of Russian Academy of Science within next year.

Metrology station for measurement and monitoring FEL radiation parameters, detector calibration, spectroscopic studies, terahertz imaging and holography.

Chemical user station for study of multi-photon processes in the interlaying metal-organic molecular beams and their ionization by mid- and far-infrared radiation. Both the fundamental laser wavelength and its 3-d and 5-th harmonics will be used in this experiment.

High energy density user station. This station is destined for the experiments, which require high power density: laser ablation, laser breakdown and CW laser discharge, aerodynamic and technology experiments.

Biological user station for study biological objects on the level of molecules, viruses, cells, and tissue.

Atmosphere study station. It is destined to study the transmission of THz radiation through the atmosphere.

VIII. Conclusion

Stable operational characteristics of the Novosibirsk free electron laser and the transmission of high power terahertz radiation through the beamline to the user facility hall indicate beginning of the conversion of the terahertz FEL from the experimental facility to the user facility. First experiments carried out on the facility have demonstrated its great potentiality for experiments in optics, high-energy-density science and other applications.

Acknowledgments

This work was supported in part by the Siberian Branch of Russian Academy of Science (grant 174/03). Experimental verification of the thermo-optical detector has been done on the CATRION facility at NSU (reg. #06-06) supported by the Ministry of Education and Science of Russian Federation.

References

[1] *V.S. Cherkassky and B A. Knyazev.* "Terahertz radiation: Last decade publications," Budker Inst. Nucl. Phys., Novosibirsk, Preprint BINP 2002-44, 2002. Available: http://www.inp.nsk.su/publications.

[2] *G.R. Neil, G.L. Carr, J. F. Gube et al,* Production of high power femtosecond terahertz radiation, Nuclear Instruments and Methods in Physics Research A, v.507, p.537–540, 2003.

[3] *E. A. Antokhin, R. R. Akberdin, V. S. Arbuzov et al*. First experimental results at the high power free electron laser at Siberian Center for Photochemistry Research, Budker Inst. Nucl. Phys., Novosibirsk, Preprint BINP 2003-53, 2003. Available: http://www.inp.nsk.su/publications.

[4] *G.R. Neil C.L. Bohn, S.V. Benson et al*. Sustained kilowatt lasing in a free-electron laser with same- cell energy recovery, Phys. Rev. Letters., v.84, p.662–665, 2000.

[5] *E.J. Minehara.* Highly efficient and high-power industrial FELs driven by a compact, stand-alone and zero-boil-off superconducting RF linac. Nuclear Instruments and Methods in Physics Research A, v.483, p.8–13, 2002.

[6] *N.G. Gavrilov, E.I. Gorniker, G.N. Kulipanov et al*. Project of CW race-track microtron-recuperator for free-electron lasers, IEEE J. Quantum Electron., v.QE-27, p.2626–28, 1991.

[7] *V.P.Bolotin, N.G. Gavrilov, D.A. Kayran et al.* The projects of high-power submillimeter-wavelength free electron laser, in "Free electron laser 2000" – Proc. 22nd Internat. Free Electron Laser Conf. and 7th FEL Workshop, Durham, USA, 2000, p.II-37–II-38.

[8] *V.V. Kubarev, G.M. Kazakevich, Y.V. Jeong, B.C. Lee*. Quasi-optical highly sensitive Schottky-barrier detector for a wide-band FIR FEL, Nuclear Instruments and Methods in Physics Research A, v.507, p.523–526, 2003.

[9] *Yu. P.Raiser*. Gas discharge physics. Moscow. Nauka, 1987 (in Russ.)

[10] *N.N. Nedialkov, S.E. Imamova, and P.A. Atanasov*. Ablation of metals by ultrashort laser pulses**,** J. Phys. D: Applied Phys., v.37**,** p.638–643, 2004.

[11] *S.P. Mickan, X.-C. Zhang*. T-ray sensing and imaging, Internat. Journ. of High Speed Electronics and Systems, v.13, p.601–676, 2003.

[12] *M.P. Golubev, A.A. Pavlov, Al.A. Pavlov, A.N. Shiplyuk*. Optical method for heat-flow registration, J. Applied Mechanics and Thechnical Physics, v.44, p.596–604, 2003.

[13] *V.S. Cherkassky, B.A. Knyazev, V.V. Kubarev et al*. Imaging techniques for a high-power THz free electron laser, in Proc. of Internat. Conf. IRMMW2004/THz2004, Karlsruhe, Germany, 2004, in print.

[14] *U. Schnars and W.P.O. Juptner*. Digital recording and numerical reconstruction of holograms, Meas. Sci. Technol., v.13, p.R85–R101, 2002.

[15] *R.J. Collier, C.B. Burckhardt, L.H. Lin*. Optical Holography, New York and London, Academic Press, 1971.

V.P. Bolotin, V.S. Cherkassky, I.K. Igumenov, D.A. Kayran, B.A. Knyazev, E.I. Kolobanov, V.V. Kotenkov, V.V. Kubarev, G.N. Kulipanov, G.L. Kuryshev, A.N. Matveenko, L.E. Medvedev, S.V. Miginsky, L.A. Mironenko, A.D. Oreshkov, V.K. Ovchar, A.K. Petrov, V.M. Popik, T.V. Salikova, S.S. Serednyakov, A.N. Skrinsky, O.A. Shevchenko, M.A. Scheglov, N.A. Vinokurov, N.S. Zaigraeva

Status of the Novosibirsk free electron laser and first experiments with high power terahertz radiation

В.П. Болотин, В.С. Черкасский и др.

Статус Новосибирского лазера на свободных электронах и первые эксперименты с мощным терагерцовым излучением

ИЯФ 2004-57

Ответственный за выпуск А.М. Кудрявцев
Работа поступила 7.09. 2004 г.

Сдано в набор 15.09.2004 г.
Подписано в печать 15.09.2004 г.
Формат 60x90 1/16 Объем 1.3 печ.л., 1.0 уч.-изд.л.
Тираж 250 экз. Бесплатно. Заказ № 57

Обработано на IBM PC и отпечатано
На ротапринте ИЯФ им. Г.И. Будкера СО РАН,
Новосибирск., 630090, пр. Академика Лаврентьева, 11